&

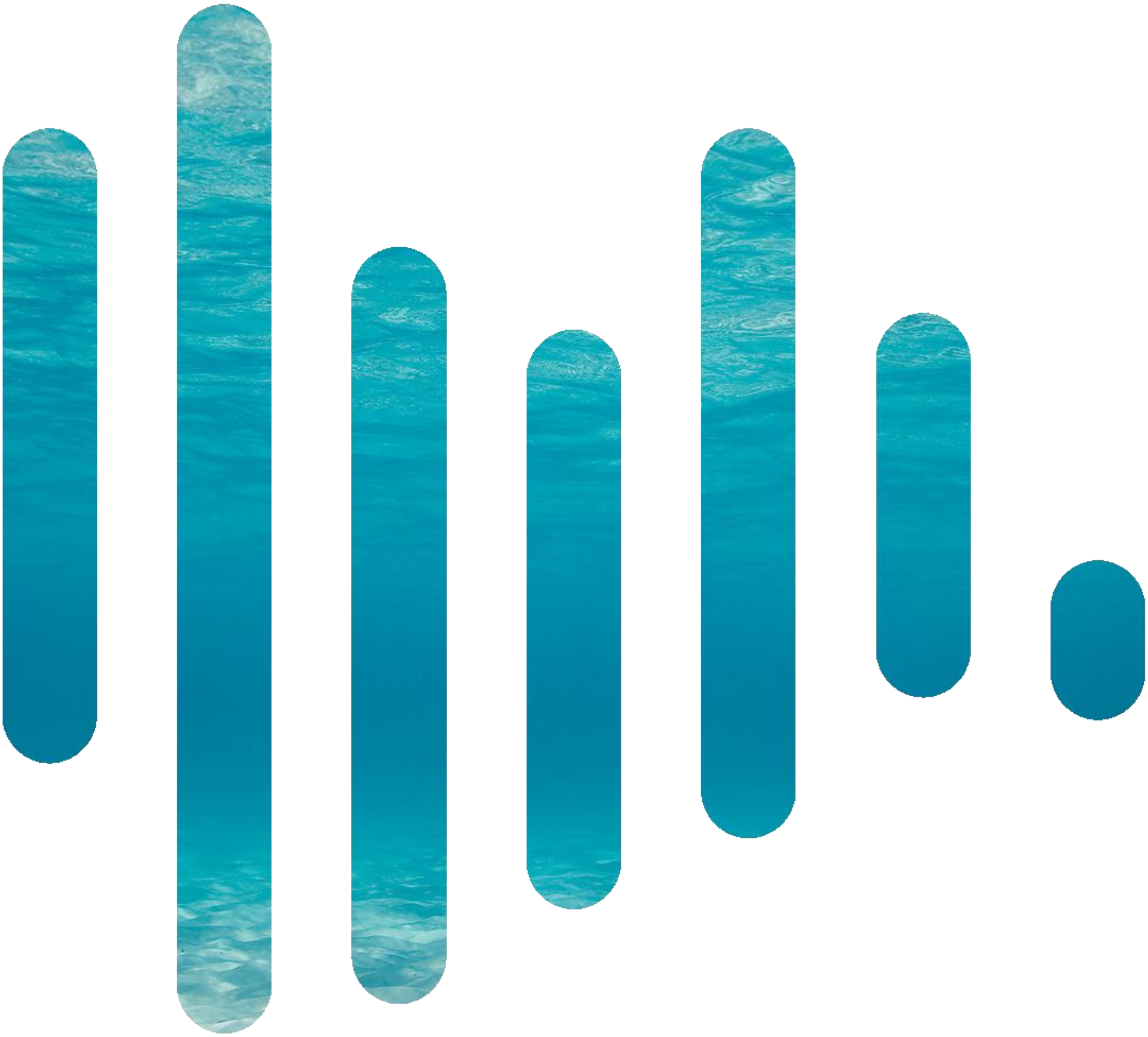

SRI Framework

Theory

Rp001 2017272 (Sound Risk Indicator)

25 March 2020

1

PROJECT: SOUND RISK INDICATOR FRAMEWORK - THEORY

PREPARED FOR: EQUINOR ASA

ATTENTION: JÜRGEN WEISSENBERGER

REPORT NO.: Rp005 2017272 (Sound Risk Indicator – Theory)

Disclaimer

This report is provided for the stated purposes and for the sole use of the named Client. Irwin Carr Ltd accepts responsibility to the Client alone that the report has been prepared with the skill, care and diligence of a competent engineer, but accepts no responsibility whatsoever to any parties other than the Client. Any such parties rely upon the report at their own risk.

Document Control

Status:	Rev:	Comments	Date:	Author:	Reviewer:
Final	2.0		25 March 2020	Rasmus Sloth Pedersen Rasmus Sloth Pedersen	Jürgen Weissenberger J. Werner

Table of Contents

1.0 MOTIVATION

Assessing the impact of underwater noise is a complicated task. There are multiple reasons for this, many of whom relate to the complexity of the marine habitats as well as the fauna within it. For an accurate assessment it is necessary to consider all these factors. We argue that this complexity can cause some confusion along with large variability in the quality of assessment, leading to potential distrust, and therefore disregard for underwater noise assessments. Given the importance of our marine resources such a scenario is highly unfavourable.

As noise propagation modelling can be a cumbersome and slow procedure, we propose the use of a **Sound Risk Indicator** (SRI) value being assigned to a noisy activity early on in the design phase. This value can be used as a guide to rapidly assess what effect changes to the activity have on the environmental acoustic impact of the activity. With changes in the activity the SRI can quickly be updated and will either increase (more noisy) or decrease (less noisy) in response to changes in activity methods. In this way the framework and associated software tool can help in planning activities while continually keeping an eye on the environmental acoustical impact changes.

This report is one part of a two-part framework:

1. **Theory (This document)**

In this document the theoretical background for a method to index noisy marine activities is described. The purpose of this document is to guide the reader through the theoretical considerations forming the background of the calculation of a Sound Risk Indicator (SRI).

2. **Suggestion for application and examples (SRI Methods)**

The methods described in this document will be applied with suggested marine animal acoustic weightings as well as examples of practical usage. The “SRI-Tool” (software package) will also be presented here.

The reader of this document is asked to remember that the sole purpose of this document is to describe the methods for calculating a Sound Risk Indicator from a rather limited information base, and not to discuss propagation losses nor the ecosystem impacts of anthropogenic noise.

1.2 ABBREVIATIONS

SRI	Sound Risk Indicator
dB	decibell, 0.1 x Bell: logarithmic unit used for sound pressure ratios
SEL	Sound Exposure Level
z-p	“zero-to-peak”
p-p	“peak-to-peak”
RMS	Root Mean Square
TL	Transmission Loss, in dB unless otherwise stated
ICC	Irwin Carr Consulting
NOAA	National Oceanic and Atmospheric Administration (of USA)
TTS	Temporary Threshold Shift
PTS	Permanent Threshold Shift
Timeseries, TS	A series of pressure values sampled with a constant time interval
dBSea	Underwater noise propagation modelling and visualisation software
SH2019	According to (Southall, et al., 2019)

2.0 INTRODUCTION

In this document we propose that with a highly simplified approach one can index noisy activities in such a way that a reduction of a calculated index value (Sound Risk Indicator, **SRI**) will result in a real-world reduction of environmental acoustic impact. We also describe the methods and considerations behind this proposal. While we repeatably use theory from the acoustic propagation modelling literature, this is *not an exercise in acoustic modelling*. The methods described here will lead to an index value (SRI), based on a relatively small amount of initial information about the environment and the sound source(s) involved.

This approach assumes a scenario where the user has limited or incomplete information about the activity, the surroundings and the presence of acoustically sensitive species.

In general, the SRI rests on a principle of quantifying the area affected by a noisy activity in a fictitious environment by using simple logarithmic spreading models and absorption. By introducing spectral information of the source, the receiver and a threshold, a corresponding range to that threshold can be calculated.
The area given by this range is used to calculate the SRI.

The use of transmission models is not an attempt to calculate real-world propagation, but solely to have a standardised way of generating an index number from initial values. The logarithmic propagation models were chosen as they ensure that SRI scales well with changes in source level and receiver sensitivity.

This document focuses on the considerations and calculation methods behind the tool.

2.1 ADDITIONAL USES

A separate use for the tool, besides the primary goal of assisting comparisons, is that we here use a propagation model that aims to find the smallest realistic transmission loss. This has the effect of providing some real-world reference to the model, and further makes real-world impacts larger than the predicted very unlikely. This is not the main purpose of the tool, but rather a consequence of the applied methods.

2.2 UNITS

Throughout this document we will strive to be consistent and strict in the use of terminology relating to units and here bring an overview of the definitions used:

Table 1. Units used throughout the report. Please see ISO 18405-2017 for more details.

Unit	Definition	Comments
dB_{RMS} ISO 18405-2017: 3.2.1.1	$dB_{RMS} = 10 \cdot Log_{10}\left(\frac{\frac{1}{t_2 - t_1} \cdot \int_{t_1}^{t_2} p(t)^2 dt}{1 \cdot 10^{-12} Pa}\right)$	Functionally equivalent to deprecated $20 \cdot Log_{10}\left(\frac{RMS}{1 \cdot 10^{-6} Pa}\right)$
$dB_{z\text{-}p}$ ISO 18405-2017: 3.2.2.1	$dB_{z-p} = 20 \cdot Log_{10}\left(\frac{Pa_{max}}{1 \cdot 10^{-6} Pa}\right)$	This assumes that Pa_{max} is equal or greater than $\sqrt{Pa_{min}}^2$
$dB_{p\text{-}p}$ ISO 18405-2017: 3.1.2.8	$dB_{p-p} = 20 \cdot Log_{10}\left(\frac{Pa_{max} - Pa_{min}}{1 \cdot 10^{-6} Pa}\right)$	Often[1] equivalent to $dB_{z-p} + 6.02\ dB$
dB_{SEL} ISO 18405-2017: 3.2.1.5	$dB_{SEL} = 10 \cdot Log_{10}\left(\frac{\int_{t_1}^{t_2} p(t)^2 dt}{1 \cdot 10^{-12} Pa}\right)$	For continuous sound this is equivalent to $dB_{RMS} + 10 \cdot Log_{10}(t_2 - t_1)$

Additional to the above units we might indicate a time associated with the unit. E.g. “$dB_{SEL\text{-}24h}$” is taken to mean the dB_{SEL} value over a 24-hour interval, “$dB_{SEL\text{-}impulse}$“ is the dB_{SEL} value of a single impulse and “$dB_{RMS\text{-}1000}$“ is the dB_{RMS} value with an averaging window of 1000 milliseconds.

[1] If pulse is below ambient pressure and compression and rarefaction phases are of equal size.

3.0 THE SOUND RISK INDICATOR

The SRI value comes from the simplified range calculation to a frequency weighted limit. The SRI is thus equal to the radius in kilometers of a circle of the same area as the area where the limit is exceeded.

For single point sources:

$$SRI = R_{Limit} \tag{1}$$

With R_{Limit} being the range to the limit. For multiple source or moving sources the SRI becomes slightly more complicated as there can be an overlap in areas from one source position and the next.

Here it is important to differentiate between two different operating modes of the SRI-tool:

1. **Geometry mode:**
   No propagation calculation takes place. The tool uses source position(s) and R_{Limit} to create a series of circles. The total area of these circles is then calculated, taking the possible overlap of one or more circles into account, so that overlapping areas are not counted more than once. No area outside the impact circle(s) is included in the basis for the SRI (Figure 1). Also, this mode ignores land.

Figure 1. Overlapping areas from two source positions.

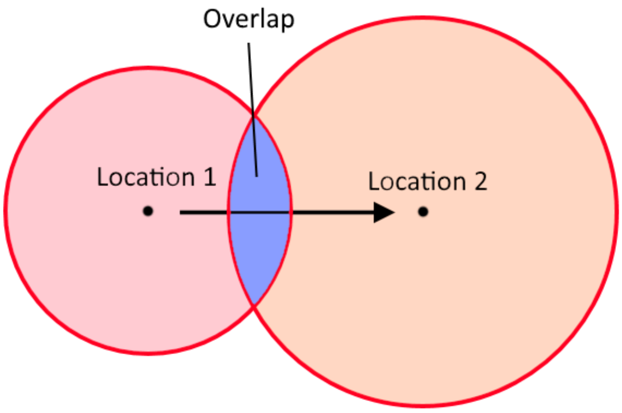

$$SRI_{Geometry-mode} = \sqrt{\frac{\sum_{i=1}^{i=n} A_{Location\ i} - A_{overlap}}{\pi}} \tag{2}$$

   With "$A_{Location\ i}$" being Area related to source location "i" and "$A_{overlap}$" the additional area from overlap. For more sources more overlaps become possible, and with e.g. four source positions, areas can overlap with areas from three other source positions and two other overlaps.

   In all cases it's the combined area that forms the base for the "Geometrical mode-SRI".

2. **Transmission Loss mode (TL-mode):**
   The tool uses the transmission loss model described in section 4.0, p. 8 to calculate levels throughout the scenario. This means that areas that fall outside the R_{Limit} for one source position, if it was alone, can be brought over the limit by contributions from other sources (Figure 2, p. 8). This effect is especially relevant for cumulative sound exposure and multiple or moving sources.

Figure 2. When calculating SRI for multiple source locations in TL mode, cumulative limit types mean that additional area will be brought over the limit. Here labelled "Additional area".

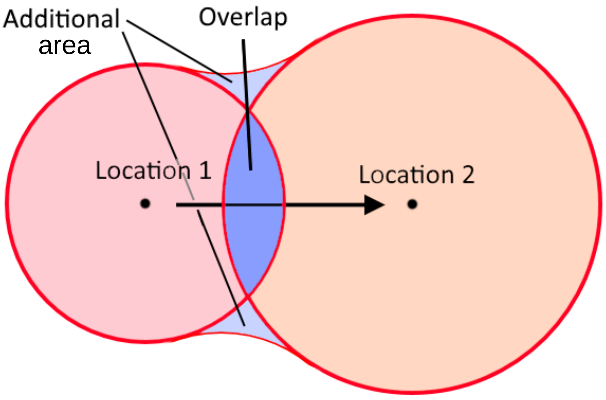

$$SRI_{TL-mode} = \sqrt{\frac{\sum_{i=1}^{i=n} A_{Location\ i} - A_{duplicate\ overlap} + A_{additional}}{\pi}} \tag{3}$$

The two operating modes will give very similar result for single sources[2], while some divergence is expected for moving sources.

The final SRI is thus the radius of a circle with an area equal to the impact area, e.g. in a simple case (Figure 2) the radius in km of a circle with the same area as the combined area of both circles and the additional area.

3.1.2 SRI from different types of limits

In the literature for marine animal impact e.g. (Carlson, Hastings, & Popper, 2007; NOAA, 2018; Popper, et al., 2014) the limits are often in two categories:

1. Cumulative impact, continuous or impulsive noises.
   Energy exposure is accumulated over time, with repeated exposures adding up to the total exposure level. Limits associated with this form of impact is given as dB_{SEL}, and often over a 24-hour time period.

2. Instantaneous impact of impulsive noises.
   The limit is given as $dB_{z\text{-}p}$ or $dB_{p\text{-}p}$. When assessing impact associated with this type of limit repeated exposures are not accumulated, and only a single impulse is assessed.

In the tool, these two noise- and limit-types are treated differently for multiple source positions as one type is for accumulated energy and the other is not. Thus multiple exposures with $dB_{z\text{-}p}$ or $dB_{p\text{-}p}$ limits yield the same SRI as for a single exposure with those limit types (as long as the source is stationary). For limit type dB_{SEL}, multiple occurrences accumulate, and thus inflate the SRI.

4.0 TRANSMISSION LOSS CALCULATION – BASE MODEL

The area/range for the SRI is determined using a simplified model based on spherical/cylindrical & absorption transmission loss with some modifications to ensure robustness across more scenario types. Below is a short overview of the background of the transmission loss model that is mostly based on work by (Duncan & Parsons, 2011), but with further additions to make their model more general.

(For details please see Duncan & Parsons (2011)[3] - they detail the adaption of the spherical/ cylindrical model described in by Urick (1983) but adopted to estimate minimal transmission loss).

[2] Provided the results grid resolution is sufficiently high (the tool will warn the user)

[3] We recommend that you read this paper, available from: https://www.acoustics.asn.au/conference_proceedings/AAS2011/papers/p87.pdf

Results from the transmission loss calculation are stored in a 3D grid of receivers that are later used when determining ranges to limits according to receiver sensitivity (section 5.3, p. 15).

Note that the model in Duncan & Parsons (2011) assumes flat (constant depth) bathymetry, while the SRI tool will use the depth at the source as a basis for calculation.

The choice of this simplistic approach was based on a desire to evaluate *minimal* transmission loss rather than *probable* transmission loss, while keeping it simple enough for fast calculations and consistent application across a wide range of scenarios.

A simple cylindrical spreading approach (TL = $10Log_{10}$(range)) will greatly underestimate transmission losses, especially for deeper water, and therefore not attractive in this framework.

A simple spherical model (TL = $20Log_{10}$(range)) was discarded for the reason that it tends to overestimate transmission losses (ignoring reflections and refraction).

The mixed model from Duncan & Parsons (2011) accounts for depth and incorporates a statistical measure to limit risk of overestimating transmission loss.

Transmission loss equation from Duncan & Parsons 2011:

$$TL = 10 \cdot Log_{10}(r) + 10 \cdot Log_{10}\left(\frac{D}{2}\right) - B + \alpha \qquad (4)$$

"TL" is transmission loss in dB, "r" is horizontal range from source in meters, "D" is depth at source location[4] in meters and "B" is a correction in dB used to adjust the probability of overestimating the transmission loss[5]. This correction is applied to counter the fact that levels are not evenly distributed in the water volume.

In calculating transmission loss for a particular range, some parts of the sound field will experience higher levels than the mean, and other parts of the sound field will experience lower levels.

It's assumed, due to the range of environmental factors that affect the exact sound field that the central limit theorem will apply, and the intensity will conform to an exponential probability distribution. Under this assumption, pressures will conform to a "Rayleigh distribution[6]", the base of this assumption is further explained in Duncan & Parsons (2011).

Solving for "r" in Eq. 4 gives the range at which a given TL is expected. By choosing this TL so that it is equal to the source level minus the limit we are interested in, a range to the limit can be found:

$$r = 10^{\left(\frac{TL + B - 10 \cdot Log_{10}\left(\frac{D}{2}\right)}{10}\right)} \qquad (5)$$

To define "B" we return to Duncan & Parsons (2011), p. 3 where they cite the results of another study (Shepherd & Milnarich, 1973) to define a probability function for a given level in the sound field exceeding the calculated mean level:

The probability that a level "I" at any point exceeds the mean level by "y" dB is then given by:

$$P_{I>y} = e^{\left(-e^{0.23026 \cdot y}\right)} \qquad (6)$$

[4] This framework uses "D" (depth) as a constant (deviating from (Duncan & Parsons, 2011)), and therefore assumes flat seabed/uniform depth.

[5] Overestimating transmission loss leads to a lower SRI

[6] A continuous probability density function characteristic of scenarios with multiple uncorrelated & normally distributed variables.

Figure 3. Plot of Eq. 6. Probability that a level is ‘y’ dB above the predicted mean level. Example call-out at suggested probability of exceedance of 1% (6.6 dB).

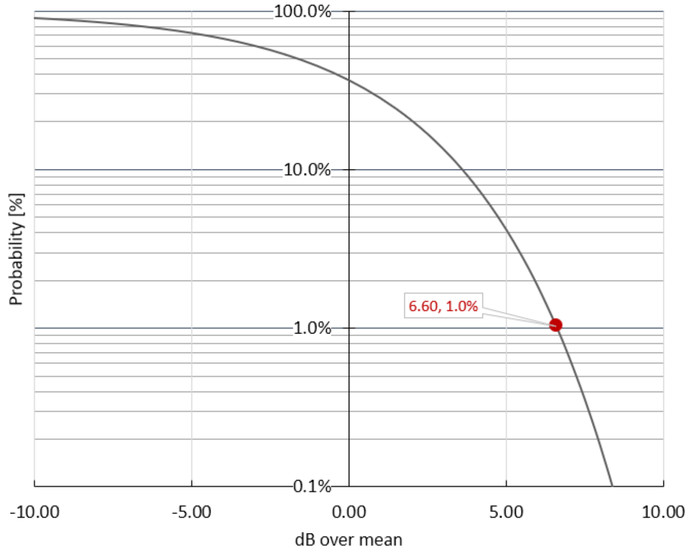

Solving Equation 6 for “y”:

$$y = \frac{\ln\left(-\ln\left(P_{I>y}\right)\right)}{0.23026} \qquad (7)$$

Setting “B” (Eq. 4 & Eq. 5) to equal “y” decreases the transmission loss according to a specified probability/risk of exceedance. We have set 1 % as this probability of exceedance. “B” will be then be 6.6 dB (set $P_{I>y}$ *in Eq. 6 to 0.01*). This reduces the transmission loss by 6.6 dB, making the impact area larger, inflating SRI.

While adding this probability of exceedance increases the complexity the calculation, we argue that it’s valuable to add a correction that addresses the fact that a simple log(range) transmission loss will under-predict some values in the sound-field, especially for impulsive sources over hard sediment (Figure 4).

We acknowledge that this approach severely *under-predicts* transmission losses for softer sediments, but argue that for a simplistic tool that aims to *index* an activity, it is desirable to work from a point of minimal theoretical transmission loss. The additional benefit is that using the tool with this propagation model will give the user an insight into a worst-case impact for the activity.

Figure 4. Effect of applying correction factor “B”. Modelling for data series “Basalt”, “Moraine” and “Sand” with dBSeaPE (Parabolic Equation method) to show effect of sediment as well as effect of changing “B”. Attenuation from absorption is ignored in this example due to the low frequencies modelled. Green line is example of a semi-spherical transmission loss with attenuation and channel leak estimated at 1.5 dB/km. The two series named “Model” are the model used in this framwork with and without the correction term “B” applied.

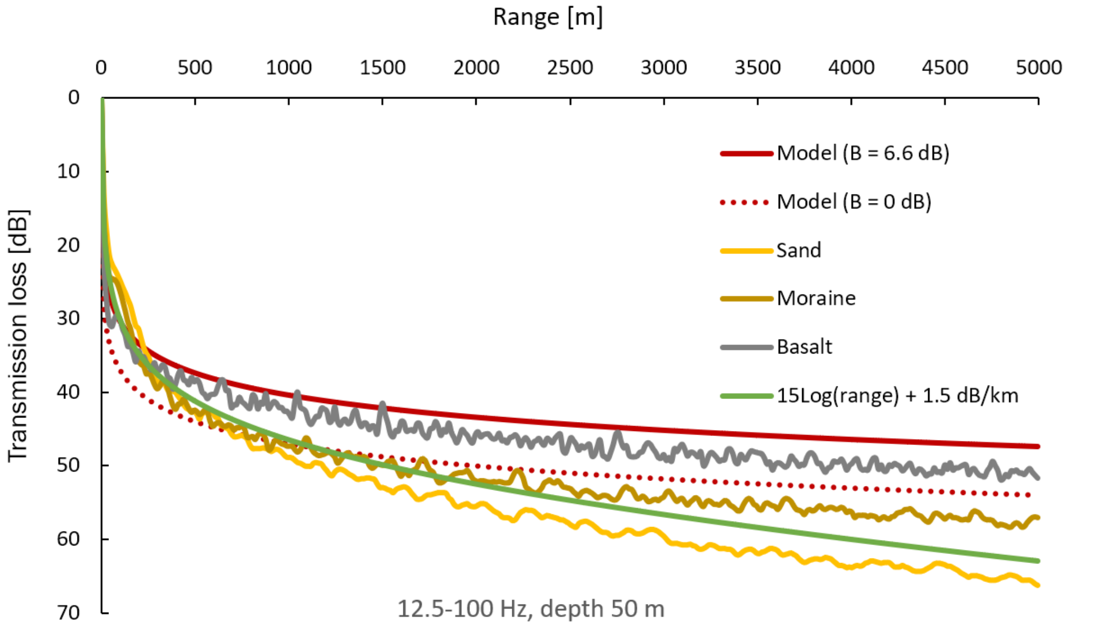

For the proponent of the noisy activity this approach can seem to unjustly associate a higher-than-realistic SRI value with the activity, but the SRI is first and foremost and index, the application to real-world scenarios is not the focus.

4.1 THE SRI TRANSMISSION LOSS MODEL

The above introduced model does not directly account for the high attenuation of high frequencies due to absorption, and further does not predict transmission losses at short ranges well. This is the basis for the following modifications to the model.

4.1.1 Absorption

Attenuation from absorption is evaluated for the centre frequency of each octave- or 3rd-octave band (depending on user choice) according to methods from (Ainslie & McColm, 1998).

4.1.2 Short Range Transmission Loss

For calculating transmission losses at short range, we introduce a modified transmission loss model. This is due to excessive transmission loss caused by the term “$10Log_{10}\left(\frac{D}{2}\right)$“ in Eq, 4, p. 10. At large depths this term will bring high transmission losses, exceeding a “$20Log_{10}(\text{range})$” model.

For example, at range 10 m and depth 500 m the transmission loss is predicted as 27 dB. This is 7 dB more than with a spherical model.

For ranges shorter than the depth we thus use the range, “*r*”, in place of the depth:

$$\begin{aligned} D > r \;\rightarrow\; TL &= 10 \cdot Log_{10}(r) + 10 \cdot Log_{10}\left(\frac{r}{2}\right) - B + \alpha \\ D < r \;\rightarrow\; TL &= 10 \cdot Log_{10}(r) + 10 \cdot Log_{10}\left(\frac{D}{2}\right) - B + \alpha \end{aligned} \tag{8}$$

“*D*”, depth at source position. “*r*”, range. “*TL*”, Transmission Loss. “*B*”, correction term (see chapter 4.0). “*α*”, absorption.

Figure 5. Comparison of transmission loss between adjusted (left) and non-adjusted model (right). For large depths the unadjusted model yields transmission losses larger than spherical spreading. The adjusted model predicts transmission losses equivalent to spherical spreading minus 10 dB until depth is larger than range.

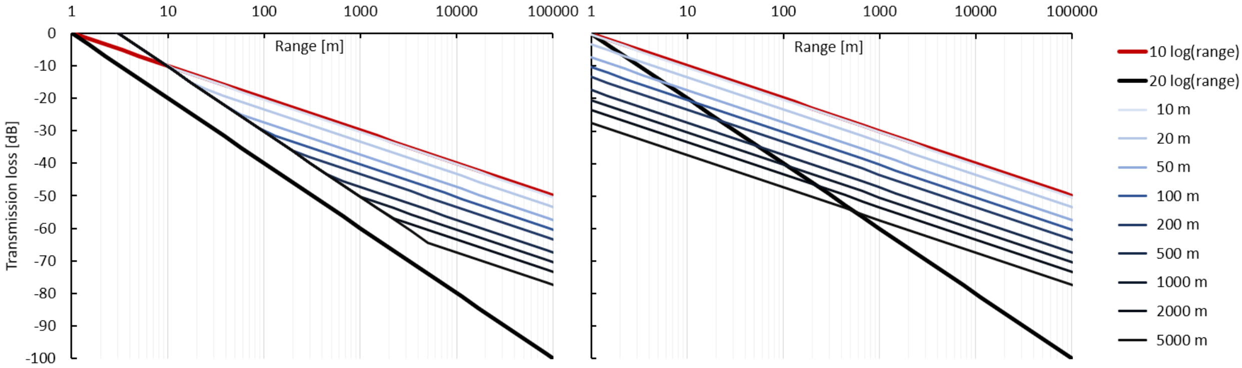

4.2 IMPULSE NOISE PROPAGATION

When impulsive noises or “transients” propagate, the actual sound pressure at any given range and depth can vary considerably from what is expected from spreading and absorption.
As an omnidirectional source (monopole) emits an impulse, that impulse will interfere with itself and give rise to volumes of higher pressure where constructive interference occurs, and correspondingly volumes where destructive interference occurs, resulting in lower pressure. As we are interested in establishing what the highest likely pressure will be, we cannot ignore this effect, and this is in part where the term “*B*” in the above section comes from (it relates to energy distribution in the water volume). Due to boundary interaction the impulse quickly becomes “stretched” in shallow scenarios and is in the tool simply modelled as any other source.

We investigated (APPENDIX I) the rate of “stretching” for an impulse in order to establish when an impulsive noise is better characterised as a continuous noise at long range due to reflections and accumulated interference (Figure 6, p. 12). We found no good model to predict this, and so a crest factor, calculated from the waveform, is applied to impulsive signals and thresholds associated with impulsive noise should be used.

It should be pointed out that under real life conditions, with many factors increasing signal degradation, we expect that for certain conditions it would be fair to characterise the received signal from a distant impulse as a continuous noise, but this is not done in this framework.

Figure 6. Boundary reflections lead to the signal being "stretched", so the energy is spread temporally with the impulse losing its initial shape.

Path	Length [m]	Time [ms]	Relative delay [ms]
1	200	133	0
2	210	140	7
3	220	147	13
4	300	200	67

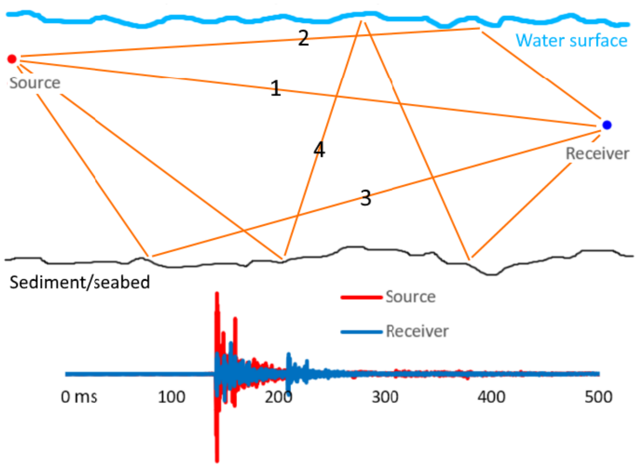

4.3 POST-PROCESSING

To go from a fully calculated sound field to an SRI-level some processing is done to interpret the results and add some conservative measures.

This will seldom change the results as semi-spherical transmission loss modelling already decreases monotonically from the source and is radially symmetrical.

4.3.1 Smoothing of results

Two methods are used to smooth results before using them to calculate the SRI: Making the results monotonically decrease and smooth the results radially. Both can be tuned by the user if they wish to do so.

Figure 7. Examples of post-processing with smoothing kernels. Left shows the application of a filter to ensure monotonically decreasing values, while the right chart is an example of a radial smoothing kernel (running mean type).

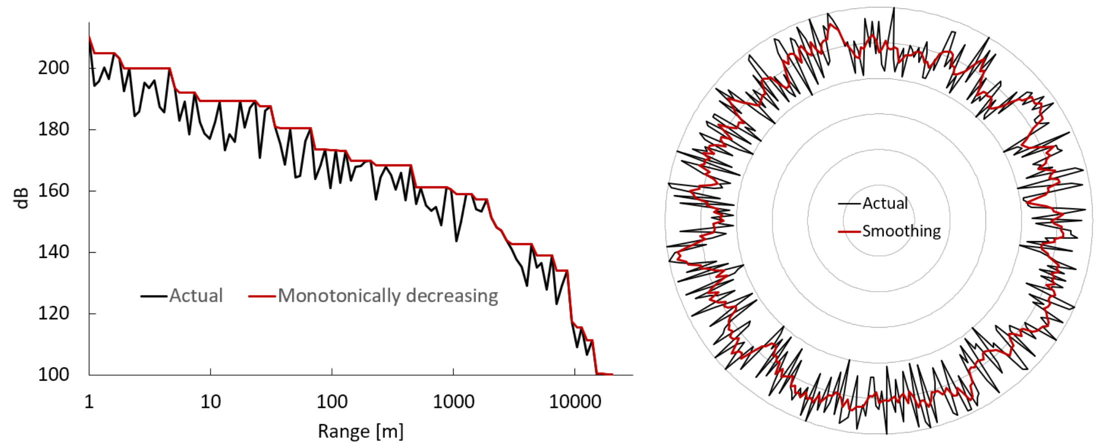

5.0 USER INPUTS

5.1 SOUND SOURCE

5.1.1 Source level and spectrum

The user can input a custom level and/or spectrum in the range 12.5 Hz to 168 kHz in octave- or 3rd octave-bands. The user can also choose from a range of predefined noise sources (e.g. generic pile driving, seismic array or a vessel) and then adjust the broadband level to match the desired level.

The source level can be entered as either dB_{SEL}, $dB_{RMS\text{-}1000}$ or as intensity, dB re 1 pW.

5.1.2 Crest factor of the source

If the source is known to contain peaks that are not captured by the $dB_{RMS\text{-}1000}$ level, the user can add information about the extent of these here. The crest factor is simply the number of dB between the maximum pressure level and the RMS-level of the sound.

$$dB_{crest\ factor} = dB_{z-p} - dB_{RMS} = dB_{p-p} - 6.02\,[7] - dB_{RMS} \tag{9}$$

If the crest factor is given by the user a $dB_{z\text{-}p}$ and $dB_{p\text{-}p}$ will be calculated from this.
The default value for the crest factor is 0 dB. Note that signal symmetry about ambient pressure is assumed unless a pressure-timeseries is loaded into the tool.

If the user knows that the source is impulsive, the option to import a timeseries into the tool should be used as this automatically will choose the correct limits and levels for the source type, as well as calculate dB_{SEL} and crest factor.

[7] Only valid if signal is symmetrical in pressure fluctuations about ambient pressure.

5.1.3 Impulsive source

For impulsive sources a timeseries (pressure vs time) can be imported (i.e. a single representative impulse from the activity).

The tool will use a filter-bank (Butterworth filters, 3rd order) to estimate the per-band dB_{SEL} level as well as $dB_{z\text{-}p}$ and $dB_{p\text{-}p}$.

Note that for the SRI tool this approach will ignore phase information in the given timeseries when applying the propagation model. The impulse is converted into a series of band levels and this is used for calculation. The crest factor from the timeseries is applied to estimate $dB_{z\text{-}p}$ and $dB_{p\text{-}p}$.

5.1.4 Simplified Seismic Source Level Calculator

For seismic sources where only the volume of the array is known we include an option to enter the array volume and the tool will calculate an equivalent point source based on this. The method is very crude by design and based on generalising data from published seismic array far-field levels (Cotton, 2003; Sutton, Jessopp, Clorennec, & Folegot, 2014). Not much information is available regarding the operation pressure of the arrays used to generate this model. Cotton 2003 states that 2000 psi was used in all 13 arrays in their study, while the Sutton et al. 2014 review uses data from a variety of sources, one of which states the operating pressure to be approximately 1900 psi. The remaining data is from field recordings where no information about operating pressure was available to the authors. While operating pressure affects the source level, there seems to be good agreement between array volume and equivalent source level in real scenarios, and so for this very simplified approach only volume is used.

Curve fitting lead to Eq. 10 that produces a $dB_{z\text{-}p}$ within 1.3 dB of the observed values (from publications mentioned above) in the frequency range 40 Hz to 63 kHz.

$$dB(V_{Ci}, f_{Hz}) = -16 \cdot \log_{10}(f_{Hz}) + 150 \cdot f_{Hz}^{-0.5} + 32.5 \cdot \log_{10}(V_{Ci}) + 100.5 \qquad (10)$$

Volume "V_{ci}" is given in cubic inches and frequency in Hz.

Figure 8. Example of a menu from the SRI software.

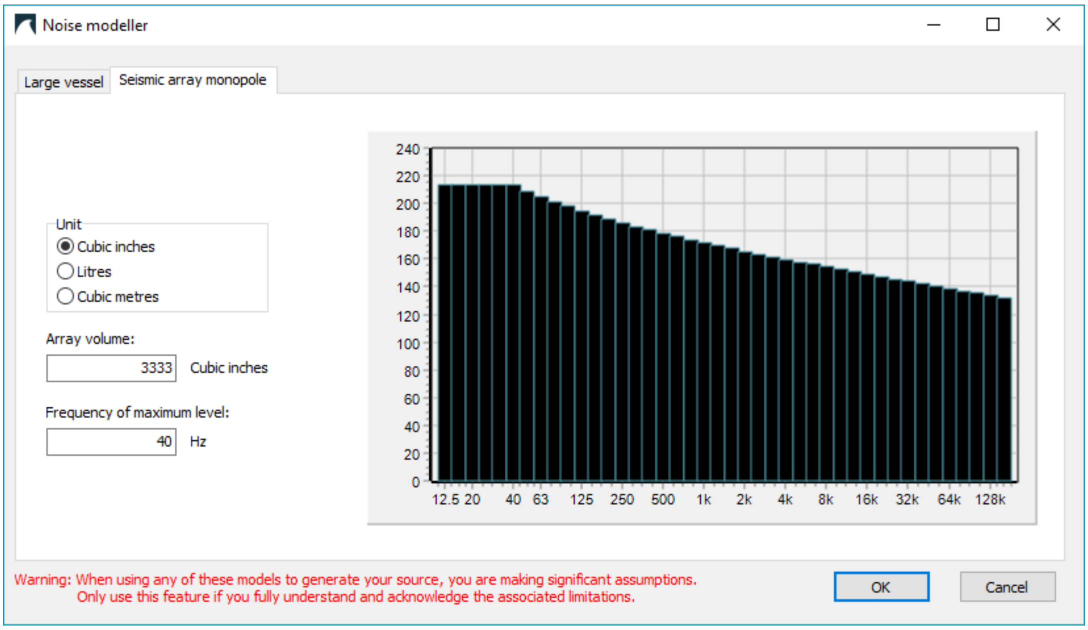

Please note that we have limited the level at the lowest frequencies. This is done as Eq. 10 generally overpredicts levels at very low frequencies (< 40 Hz), frequencies that would otherwise have a large impact on the calculated impact ranges.

5.1.5 Large vessel noise model

Additionally, we have implemented a source generator for large vessels following the model by (Wittekind, 2014) to facilitate use of realistic sound sources, should the user not have their own data. This model takes input about the vessel and engine size along with design information about operating speeds and engine mounting method.

Figure 9. Example of a menu letting the user generate a large vessel noise source.

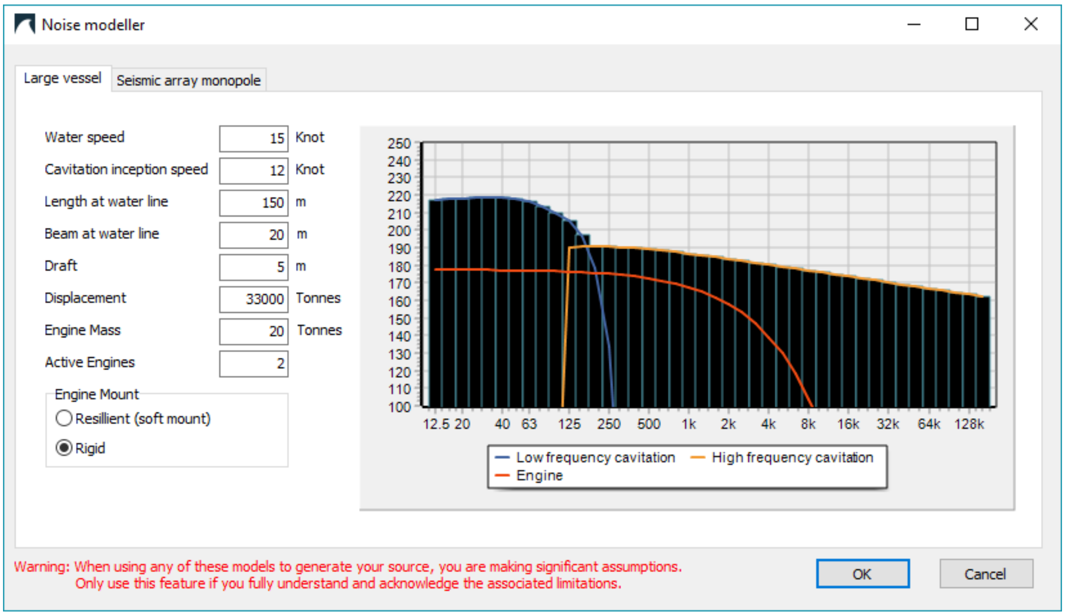

5.2 ENVIRONMENT AND SCENARIO

The user has options to include a limited amount of information about the environment of the proposed activity.

5.2.1 Bathymetry

The user can specify the bathymetry of the scenario by importing data files containing depth information or generate their own representative scenario.

5.2.2 Frequency range and absorption

To estimate absorption from magnesium sulphate and boric acid equations from (Ainslie & McColm, 1998) are used. The user can further specify water temperature and pH, but this will only affect results marginally.

Frequency range is determined by the user – 12.5 Hz to 168 kHz is available.

5.3 RECEIVERS AND LIMIT TYPES

Besides the source level and spectrum and transmission loss, the receiver's limit and frequency specific sensitivity is what determines the SRI value.

The tool is set up to either use no acoustic weightings or to apply acoustic weightings to the results prior to using a limit to calculate an area. Weightings should here be understood similarly to e.g. A-weightings for humans, in that they are not directly related to the hearing threshold, but rather mimics the general form. Their application yields a weighted noise spectrum, dB(A) for an A-weighted noise level. In the separate report "Methods for the SRI-tool" we introduce a range of suggested weightings covering marine macro-fauna, and here we will only go through the method of applying multiple weightings and limits rather than justify the choice of any specific weightings.

5.3.1 Receiver weightings and limits

We will use two species groups, "Low" and "High" to illustrate how we apply weightings and limits. In this framework we have adopted the equations from the work by NMFS and NOAA (NOAA, 2018), as it allows us to have a consistent approach to all hearing groups using the general equation on page 13 of the guidance document (NOAA, 2018). Note that the weightings suggested by Southall et al in 2019 are identical to these, only the naming differs (Southall, et al., 2019).

$$E(f) = K - 10 \cdot \log_{10}\left(\frac{\left(\frac{f}{f_1}\right)^{2a}}{\left(1+\left(\frac{f}{f_1}\right)^2\right)^a \cdot \left(1+\left(\frac{f}{f_2}\right)^2\right)^b}\right) \tag{11}$$

"E" is a detection limit in dB$_{RMS\text{-}1000}$ at a specified frequency. "K" is a vertical offset to adjust the minimum weighting level. "a" determines low-frequency roll-off in sensitivity (20 · a dB/decade). "b" determines high-frequency roll-off in sensitivity (20 · b dB/decade). Lower and higher "limit" of best hearing are given by "f_1"and "f_2".

After received levels have been determined across the scenario, weightings for each included receiver type are applied to find weighted broadband levels throughout the scenario. Weightings are applied for the centre frequency of either octave- or 3rd-octave bands.

Specific group limits are evaluated against the group-weighted broadband level to establish the range to the limit.

Figure 10. Example of two weightings (Eq. 11) being applied to a 3rd octave band spectrum. Levels given in legend are broadband levels while axes show band levels or weighting levels.
Top left: Weightings. Top right: Source. Bottom: weighted level.

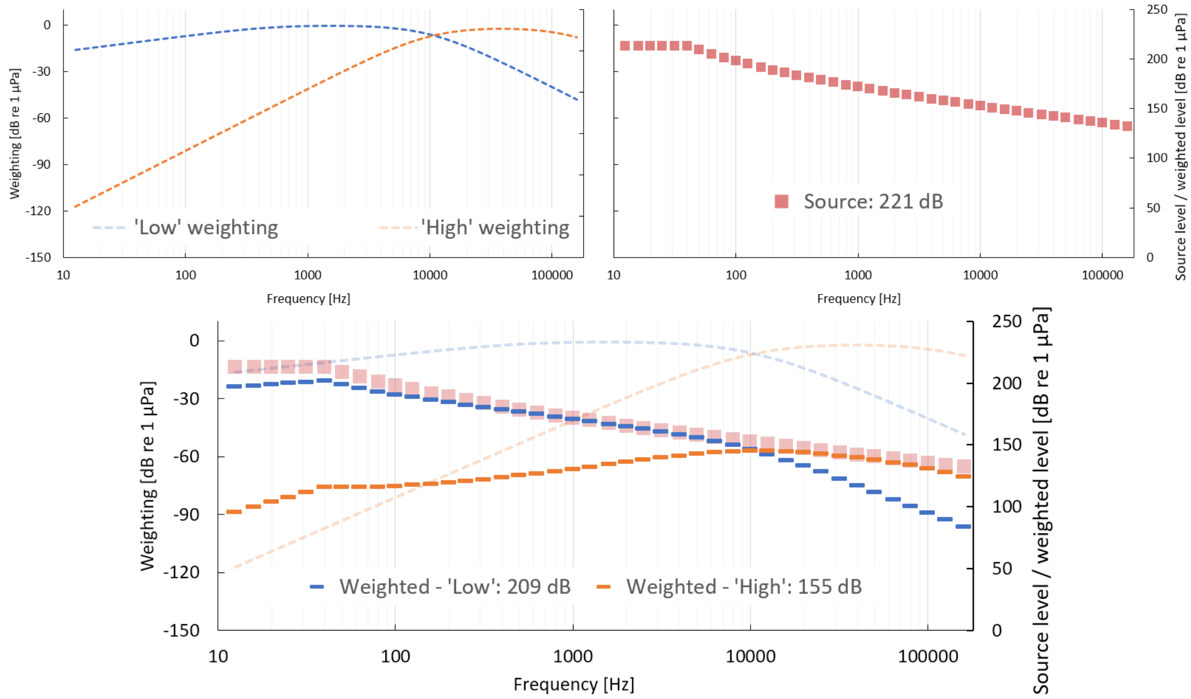

If we set limits for group "Low" and "High" to be 170 dB and 160 dB respectively, we will see that even though group "High" has a lower limit of 160 dB, the weighting means that the limit is not exceeded (Figure 10 above & Table 2 below). The range to the limit of "Low" is ~725 m, leading to an SRI of 0.73 for the "Low" group. The group "High" here has an SRI of "0".

Table 2. Overview of "Low" and "High" group limits and weighted levels.

Group	Limit [dB$_{SEL}$]	Weighted level [dB$_{SEL}$]	Limit exceeded?
Low	170	209	Yes (39 dB)
High	160	155	No (-5 dB)

Please see the "SRI Methods" document for real world examples.

6.0 CONCLUDING REMARKS

The example above concludes this report, describing the theory of the framework used to compress and integrate noisy activity information into a single Sound Risk Indicator. It is not intended as a replacement for impact assessments, but rather to serve as an indexing tool to let industry and regulators easily compare various scenarios by assigning a single number to them.

We invite readers of this document to send comments and questions to:

Rasmus Sloth Pedersen

Rasmus Sloth Pedersen
rasmus.pedersen@irwincarr.com

7.0 REFERENCES

Ainslie, M., & McColm, J. (1998). A simplified formula for viscous and chemical absorption in sea water. *Journal of the Acoustical Society of America, 3*(103), 1671-1672.

BOEM. (2014). *Fish Hearing and Sensitivity to Acoustic Impacts.* Convention on Biological Diversity - UN Environment.

Carlson, T., Hastings, M., & Popper, A. (2007). *Update on recommendations for revised interim sound exposure criteria for fish during pile driving activities.* Olympia: Washington Department of Transportation.

Christensen-Dalsgaard, J., Brandt, C., Willis, K. L., Christensen, C. B., Ketten, D., Edds-Walton, P., . . . Carr, C. E. (2012). Specialization for underwater hearing by the tympanic middle ear of the turtle, Trachemys scripta elegans. *Proceedings of the Royal Society B*, 1-9.

Cotton, R. (2003). *Seismic source analyses for The SeaScan Tri-Cluster® seismic sound source system. Final Report.* Dunelm Enterprises Inc.

DFO Canada. (2006). *Effects of Seismic Energy on Fish: A Literature Review.* Dartmouth: Department of Fisheries and Oceans. Retrieved from http://waves-vagues.dfo-mpo.gc.ca/Library/328787.pdf

Duncan, A. J., & Parsons, M. J. (2011). How Wrong Can You Be? Can a Simple Spreading Formula Be Used to Predict Worst-Case Underwater Sound Levels? *87*.

Fisher, F., & Simmons, V. (1977). Sound absorption in seawater. *Journal of the Acoustical Society of America*(62), 558-564.

Jensen, F., Kuperman, W., Porter, M., & Schmidt, H. (2011). *Computational Ocean Acoustics* (2nd ed.). Springer.

Ketten, D. R. (1995). Estimates of blast injury and acoustic trauma zones for marine mammals from underwater explosions. *Sensory Systems of Aquatic Mammals*, 391-407.

Ketten, D. R., & Bartol, S. M. (2005). *Functional Measures of Sea Turtle Hearing.* Boston: Office of Naval Research.

KJ, M., SC, A., & JC, G. (2012). Underwater hearing in the loggerhead turtle (Caretta caretta): a comparison of behavioral and auditory evoked potential audiograms. *Journal of Experimental Biology*, 3001-3005.

Lombarte, A., Yan, H., Popper, A., Chang, J., & Platt, C. (1993). Damage and regeneration of hair cell ciliary bundles in a fish ear following treatment with gentamicin. *Hearing Research*, 166-174.

Mann, D., higgs, D., Tavolga, W., Souza, H., & Popper, A. (2001). Ultrasound detection by clupeiform fishes. *Journal of the Acoustical society of America*, 3048-3054.

Menot, A. V. (2009). Continental margins between 140m and 3500m depth. IFREMER http://www.marineregions.org/. Retrieved from IFREMER: http://www.marineregions.org/downloads.php#comarge

NOAA. (2016). *Guidance for Assesing the Effects of Anthropogenic Sound on Marine Mammal Hearing.* National Oceanic and Atmospheric Administration.

NOAA. (2018, 02 19). *NOAA Fisheries*. Retrieved from West Coast Region >> Marine Mammals: http://www.westcoast.fisheries.noaa.gov/protected_species/marine_mammals/threshold_guidance.html

Piniak, W., Eckert, S., Harms, C., & Stringer, E. (2012). *Underwater hearing sensitivity of the leatherback sea turtle (Dermochelys coriacea): Assessing the potential effect of anthropogenic noise.* Herndon: BOEM.

Piniak, W., Mann, D., Harms, C., Jones, T., & Eckert, S. (2016). Hearing in the Juvenile Green Sea Turtle (Chelonia mydas): A Comparison of Underwater and Aerial Hearing Using Auditory Evoked Potentials. *PLos ONE*, 1-14.

Popper, A. N., Hawkins, A. D., Fay, R. R., Mann, D. A., Bartol, S., Carlson, T. J., . . . Zeddie, D. G. (2014). *Sound Exposure Guidelines for Fishes and Sea Turtles. A Technical Report prepared by ANSI-Accredited Standards Committee S3/SC1 and registered with ANSI.* London: Springer.

Popper, A., Carlson, T., Hawkins, A., Southall, B., & Gentry, R. (2006). *Interim criteria for injury of fish exposed to pile driving operations: A white paper.* Olympia: Washington State Department of Transportation.

Popper, A., Smith, M., Cott, P., Hanna, B., MacGillivray, A., Austin, M., & Mann, D. (2005). Effects of exposure to seismic airgun use on hearing of three fish species. *Journal of the Acoustical Society of America*, 3958-3971.

Shepherd, W., & Milnarich, P. (1973). Basic relations between a Rayleigh-distributed randomly varying voltage and a decibel record of the voltage. *Proceedings of the IEEE*, 1765-1766.

Smith, M. E. (2008). TESTING THE EQUAL ENERGY HYPOTHESIS IN NOISE-EXPOSED FISHES. *Bioacoustics*, 343-345.

Smith, M. E., Kane, A. S., & Popper, A. N. (2004). Acoustical stress and hearing sensitivity in fishes: does the linear threshold shift hypothesis hold water? *The Journal of Experimental Biology*, 3591-3602.

Smith, M., Coffin, A., Miller, D., & Popper, A. (2004). Anatomical and functional recovery of the goldfish (Carassius auratus) ear following noise exposure. *Journal of Experimental Biology*, 4193-4202.

Southall, B. L., Bowles, A. E., Ellison, W. T., Finneran, J. J., Gentry, R. L., Jr., C. R., . . . Tyack, P. L. (2007). Marine Mammal Noise Exposure Criteria: Initial Scientific Recommendations. *Aquatic Mammals*, i-509.

Southall, B. L., Finneran, J. J., Reichmuth, C., E.Nachtigall, P., Ketten, D. R., Bowles, A. E., . . . Tyack, P. L. (2019). Marine Mammal Noise Exposure Criteria:Updated Scientific Recommendations for Residual Hearing Effects. *Aquatic Mammals*, 125-232. doi:10.1578/AM.45.2.2019.125

Subacoustec. (2004). *Fish and Marine Mammal Audiograms: A summary of available information.* Hampshire: Subacoustech Ltd.

Sutton, G., Jessopp, M., Clorennec, D., & Folegot, T. (2014). *STRIVE, Mapping the Spatio-temporal Distribution of Underwater Noise in Irish Waters.* Wexford, Ireland: Environmental Protection Agency.

United Nations Environment Programme. (2008). *In Dead Water – Merging of climate change with pollution, over-harvest, and infestations in the world's fishing grounds.* Norway: GRID-Arendal https://gridarendal-website-live.s3.amazonaws.com/production/documents/:s_document/237/original/InDeadWater_LR.pdf?1487681947.

Urick, R. (1983). *Principles of Underwater Sound, 2nd edition.* ISBN 0-932146-62-7: Peninsula Publishing.

Wittekind, D. K. (2014). A Simple Model for the Underwater Noise Source Level of Ships. *Journal of Ship Production and Design*, 1-8.

Appendix I – Sound impulsivity.

When an impulse propagates through an environment it undergoes self-interference. This process works to "stretch" the impulse, meaning that a receiver will be exposed to a lengthened and "smeared out" version of the initial impulse. We here present the background for investigating whether this effect can be generalised to calculate a range at which the impulse is so stretched that it is better characterised as a continuous noise. All calculations assume that the sound speed is constant, depth is constant, that there is no absorption and there is perfect reflection at boundaries (air-water interface inverts signal).

1 ESTIMATION OF PROPORTION OF WAVEFRONT THAT HAS BEEN REFLECTED

In a scenario with perfectly reflecting sea surface and sediment we can calculate the proportion of a wave-front that arrives at a range without having been reflected (Figure 11 & Eq. 1 & 2). This is interesting as the initial wavefront will experience at least spherical spreading loss (Eq. 1), a rate of attenuation much greater than the "spherical-cylindrical" approach often used (Eq. 2).

$$TL_{sph} = 20 \cdot \log_{10}(range) \tag{1}$$

$$TL_{s+c} = 10 \cdot \log_{10}(range) + 10 \cdot \log_{10}(k) \tag{2}$$

"TL_{sph}", spherical transmission loss; "TL_{s+c}", spherical-cylindrical transmission loss; "k", transition range where transmission loss goes from spherical to cylindrical.

Proportion of wavefront reflected at least once, assuming flat bathymetry:

$$R_1 = 1 - (fraction\ not\ reflected\ from\ surface) - (fraction\ not\ reflected\ from\ bottom)$$

$$R_1 = 1 - \frac{\sin^{-1}\left(\frac{S_D}{R_h}\right) - \sin^{-1}\left(\frac{D - S_D}{R_h}\right)}{\pi} \tag{3}$$

For spreadsheet:

```
"=1-IF(Rh>SD,ASIN(SD/Rh)/PI(),0.5)-IF(Rh>(D-SD),ASIN((D-SD)/Rh)/PI(),0.5)"
```

The "ASIN" function does not tolerate inputs ≥ 1 so IF-statements are necessary.

"R_1" being proportion of wave-front that has been reflected at least once, "S_D" is source depth, "R_h" is horizontal range from source, "D" is depth at source.

Equation (1) above can be expanded to accommodate more reflections:

$$R_{n_{rfl}} = 1 - \frac{\sin^{-1}\left(\frac{S_D + D(n_{rfl} - 1)}{R_h}\right) - \sin^{-1}\left(\frac{D - S_D + D(n_{rfl} - 1)}{R_h}\right)}{\pi} \tag{4}$$

For spreadsheet:

```
"=1-IF(Rh>SD+D*(nrfl-1),ASIN((SD+D*(nrfl-1))/Rh)/PI(),0.5)-IF(Rh>(D-SD+D*(nrfl-1)),ASIN((D-SD+D*(nrfl-1))/Rh)/PI(),0.5)"
```

"R_{nrfl}" (n-reflections) is the proportion of the wavefront that has been reflected "n_{rfl}" times. From the above we can establish that, at a range equal to 5 times the depth:

94 % of the wave-front has been reflected at least once (meaning 6 % has not been reflected at all).

80-81 % has been reflected at least twice.

66-67 % has been reflected at least thrice.

50-51 % has been reflected at least four times.

20-29 % has been reflected at least five times.

Table 3. Example of application of Eq. 2 to calculate the proportion of a wave-front that has experienced a given number of reflections at a given distance. The distance is given as Range/Depth as the results are dependent on that ratio rather than their absolute values.

		Range/Depth							
		0.10	0.50	1.00	2.00	2.50	3.15	4.0	5.0
Number of reflections experienced by wave-front	0	91%	67%	38%	16%	13%	10%	8%	6%
	1	9%	33%	62%	41%	29%	22%	17%	13%
	2	0%	0%	0%	42%	45%	28%	19%	14%
	3	0%	0%	0%	0%	14%	37%	27%	16%
	4	0%	0%	0%	0%	0%	3%	29%	24%
	5	0%	0%	0%	0%	0%	0%	0%	26%
Sum		100%	100%	100%	100%	100%	100%	100%	100%

Figure 11. Schematic of a wave-front moving away from a source, when bounded by two perfectly reflecting surfaces (8 time-snapshots). Yellow arcs are direct part of original impulse, red arcs have been reflected once, purple arcs twice and blue arcs thrice. Point “A”, at range equal to source depth, no part of the impulse arriving here at this time has been reflected and the impulse retains its original “form”. Point “B”, at range equal to source depth minus total depth, this is the maximal possible range for not having any part of the wave-front being reflected (in the case of source depth = total depth/2). Point “C”, range equal to depth, 50-67 % of the wave-front has now been reflected at least once. Point “D”, range equal to 2 x total depth, 83-84 % of the initial wave-front has now been reflected at least once. At point “D”, a maximum of 17 % of the wave-front has arrived directly, with no reflections.

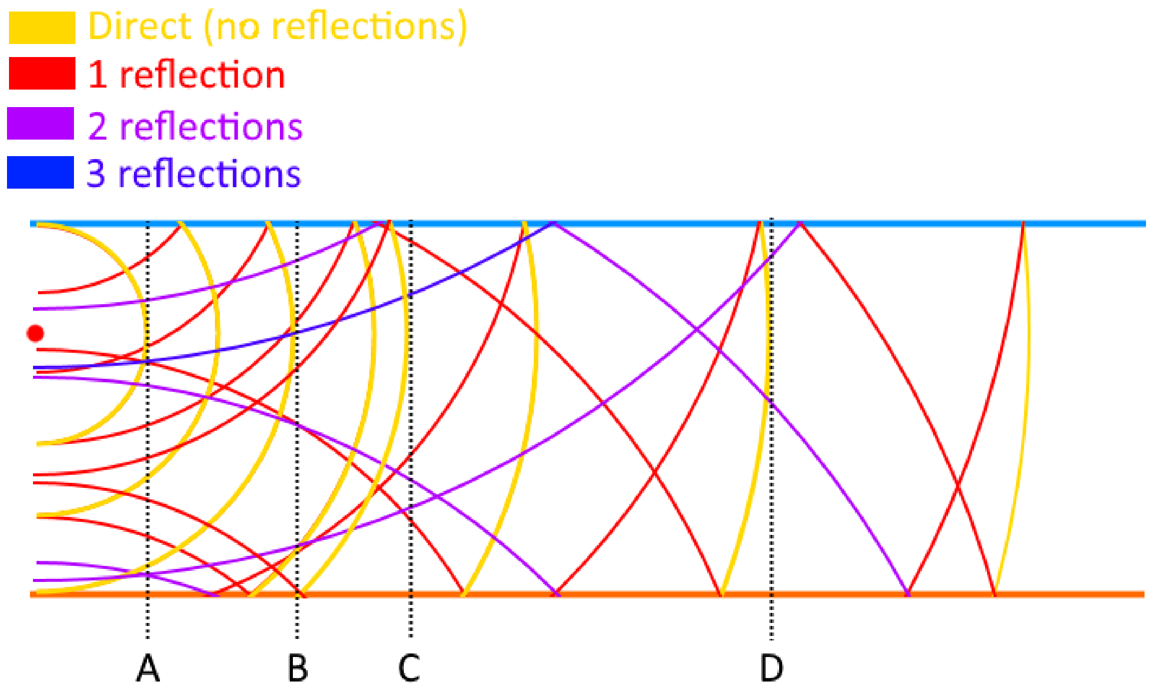

On the basis of the above, we speculated that as only the initial wavefront retains its original shape, but with a high transmission loss of > 20 x $\log_{10}$(range), a receiver at a range of 5x depth would experience the impulse as a series of smaller impulses with peak pressures as predicted by spherical spreading, but exposure as predicted by Eq. 2. We hoped to use this approach to investigate how the crest factor ($dB_{z\text{-}p}$-dB_{RMS}, as a proxy for impulsiveness) developed with increasing number of reflections and range.

The definition of impulsiveness in the literature is precariously ambiguous:

ISO 1996-1:2016 (3.5) states that:
"At the time of publication of this part of ISO 1996, no mathematical descriptor exists which can define unequivocally the presence of impulsive sound or can separate impulsive sounds into the categories given in 3.5.1 to 3.5.3."

The British standard "BS 4142:2014" defines impulsiveness by the use of dB_{RMS} with a 50 ms window and the change in tangent slope versus time (10 dB/second). This is however unsuitable for our application, as a 50 ms integration window is too slow to represent the very short integration times found especially in marine mammals. This line of investigation was abandoned as the 10 dB/second limit proved unrealistic for integration times shorter than 50 ms.

We then looked to get to a crest factor less than 6 dB, but this was also unrealistic, and so this approach abandoned.

This leads to the next section where we calculate the travel times for a seismic source impulse and sample the resulting sound field.

2 ESTIMATING TIME DELAY FROM RAY PATHS

By calculating the length of various transmission paths, we can calculate the relative arrival time of an emitted impulse and thereby investigate the received time-pressure signal considering interference. We assume no refraction in the following.

For a sound to be reflected e.g. three times it has bounced of the boundaries (surface & sediment) three times (the order depending on weather it hit the surface or the sediment first. (Figure 16 C).

Those bounces lead to a minimal additional distance to travel when compared to a path that hasn't bounced.

First, let's calculate the length of the direct path:

$$Direct\ Path = \sqrt{(S_D - R_D)^2 + {R_h}^2} \tag{5}$$

"S_D" source depth, "R_D" receiver depth and "R_h" horizontal range. Any path other than the direct will have travelled longer due to its path travelling to either boundary (surface or sediment) at least once. The length of that path can be similarly calculated:

$$Odd\ Bounce\ Path = \sqrt{(S_D + R_D + n_B \cdot D - D)^2 + {R_h}^2} \tag{6.1}$$

$$Even\ Bounce\ Path = \sqrt{(S_D - R_D + n_B \cdot D)^2 + {R_h}^2} \tag{6.2}$$

"D" being depth, "R_h" is horizontal range and "n_B" is number of bounces.

Note that "S_D" and "R_D" are source distance to boundary of first reflection and can be either surface or bottom.

The shortest path with three bounces (or any odd number) exists when S_D and R_D approach the same boundary (either surface of bottom) and their distance to that boundary decreases towards zero (Figure 16 C), meaning that the shortest path with n_B bounces at limit is:

$$Bounces\ Shortest\ Path = \sqrt{\left((n_B - 1) \cdot D\right)^2 + {R_h}^2} \tag{7}$$

Figure 12. Ray paths for two to four bounces. Notice that as the source (red) and the receiver (blue) move in direction of the arrows, their shortest path length becomes equal to that of the longest path with 2 fewer bounces.

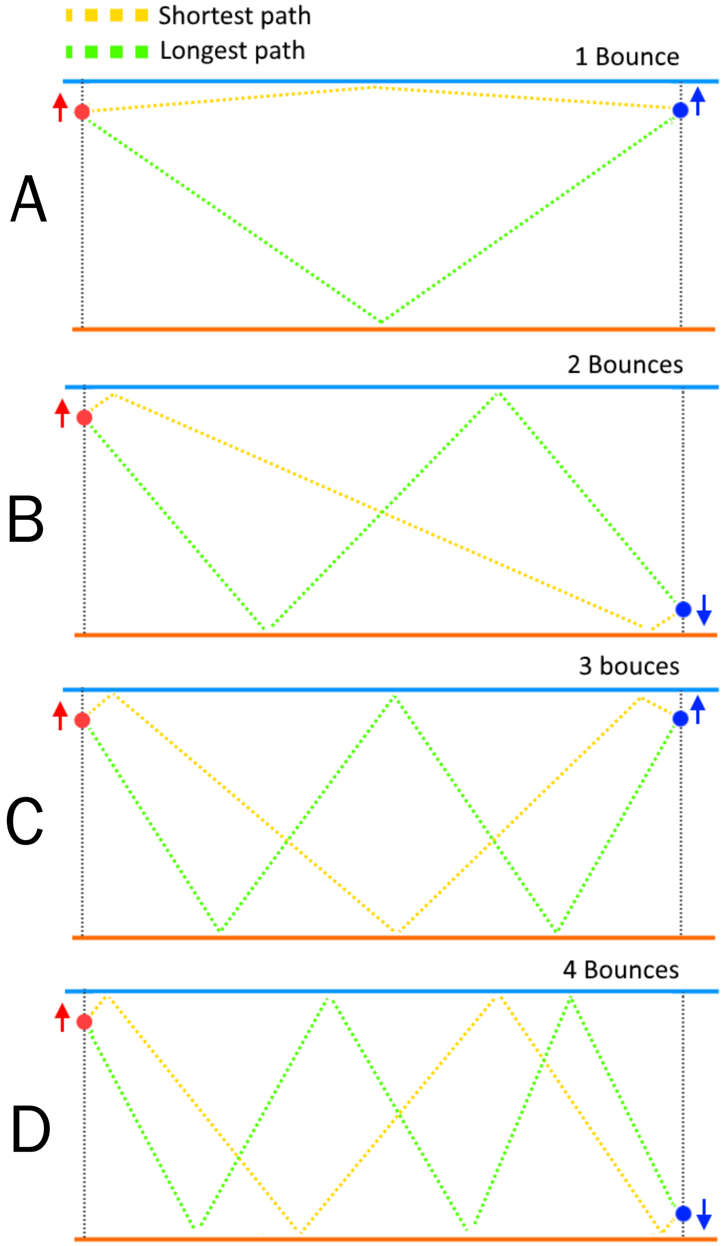

For an even number of bounces the situation is slightly different in that the shortest path for an even number of bounces exists when the source and the receiver are at opposite boundaries (Figure 16 B & D). This however, results in the same relationship as for odd bounces (Eq. 7). See Figure 16 to graphically confirm this, keeping Pythagoras' theorem ($a^2+b^2=c^2$) for right-angle triangles in mind.
For the direct path, with the same source and receiver depths, equation (5) reduces to R_h (as the term $(S_D-R_D)^2$ becomes zero when $S_D = R_D$):

$$Direct\ Path = \sqrt{{R_h}^2} = R_h \tag{8}$$

With the shortest direct path equal to R_h and the corresponding shortest bounce path from Eq. 7 we can estimate the *factor* with which the direct path relates to the reflected path.

$$F_{n_B} = \frac{\sqrt{(n_B - 1) + \left(\frac{R_h}{D}\right)^2}}{\left(\frac{R_h}{D}\right)} = \frac{R_{reflected}}{R_{direct}} \tag{9}$$

In the worst-case scenario[8] R_{direct} is equal to R_h (Figure 16 A) and we can calculate the additional travel and thereby the impulse delay "I_d" in milliseconds by modifying Eq. 9 slightly:

$$I_d(R_h, D, n_B) = R_h \cdot \left(\frac{\sqrt{(n_B - 1) + \left(\frac{R_h}{D}\right)^2}}{\left(\frac{R_h}{D}\right)} - 1 \right) \cdot \frac{1500\, {}^{m}/_{s}}{1000\, {}^{ms}/_{s}} \tag{9.1}$$

We are now almost in a position to generalise delay times for impulses at any range and depth.

For example, at a horizontal range of 1000 meters:

Table 4. Application of Eq. 9.1 to calculate *shortest possible* delay between first arrival and arrival of subsequent rays. "Dist" is distance travelled for that particular path. The horizontal range is 1000 meter throughout.

Extra distance & delay from reflections		Reflections									
		1		2		3		4		5	
R_h [m]	1000	Dist [m]	Time [ms]	Dist [m]	Time [ms]	Dist [m]	Time [ms]	Dist [m]	Time [ms]	Dist [m]	Time [ms]
Depth [m]	10000	0	0	9050	6033	13177	8785	16349	10900	19025	12683
	2000	0	0	1236	842	2000	1333	2606	1737	3123	2082
	1000	0	0	414	576	732	488	1000	667	1236	824
	500	0	0	118	79	225	150	323	215	414	276
	333	0	0	54	36	106	70	155	103	202	135
	250	0	0	31	21	61	40	90	60	118	79
	200	0	0	20	13	39	26	58	39	77	51
	100	0	0	5	3	10	7	15	10	20	13
	10	0	0	0	0	0	0	0	0	0	0

We can visualise this by splitting the impulse into rays, apply a delay and transmission loss, and then add them up at a receiver location, see Figure 17 below.

[8] Small difference in arrival time is worst case for summation of energy over a short time duration.

Figure 13. Example of tracking the first 11 paths from source to receiver (as straight lines, with perfect reflection at boundaries). Range 1000 m, depth 200 m, source depth 5 m, receiver depth 50 m. The source is a 4000 Cui seismic array (thin red line). Notice that the crest factor (CF $dB_{z\text{-}p}$ - dB_{RMS}) is 18.7 dB at the source, but 9.3 dB at the receiver 1 km away (thick red line). Red lines read on right axis (dB), remaining lines on left axis (Pa).

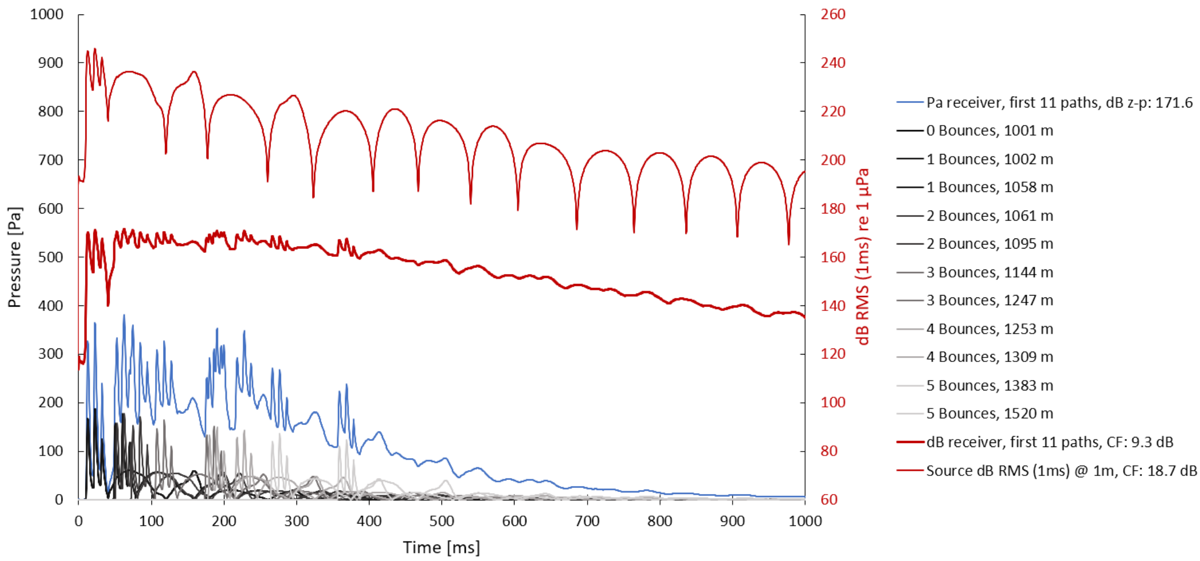

Taking this a little further, below are the first 41 paths (0-20 reflections). We see that even though the energy gets spread out over a longer duration the signal retains a high crest factor, and so by our own standards remains impulsive. The following 5 charts show various metrics relating to the received signal in 1800 different cases: 20 different ranges, 10 scenario depths and 9 receiver positions (depths) at those ranges. The mean of the 9 receiver depths and 95 % confidence interval is plotted versus the associated horizontal range. Range "0" is zero meters horizontally, not slant range (this explains the large variation a 0 m). Notice that even though "Peak" decreases quicker than "RMS" and "SEL" and the duration of 90 % of the energy is > 1 second for most depths and ranges the crest factor remains high (> 20 dB). We therefore cannot justify treating the signal as a continuous signal and must continue to use appropriate impulsive thresholds when assessing impulses.

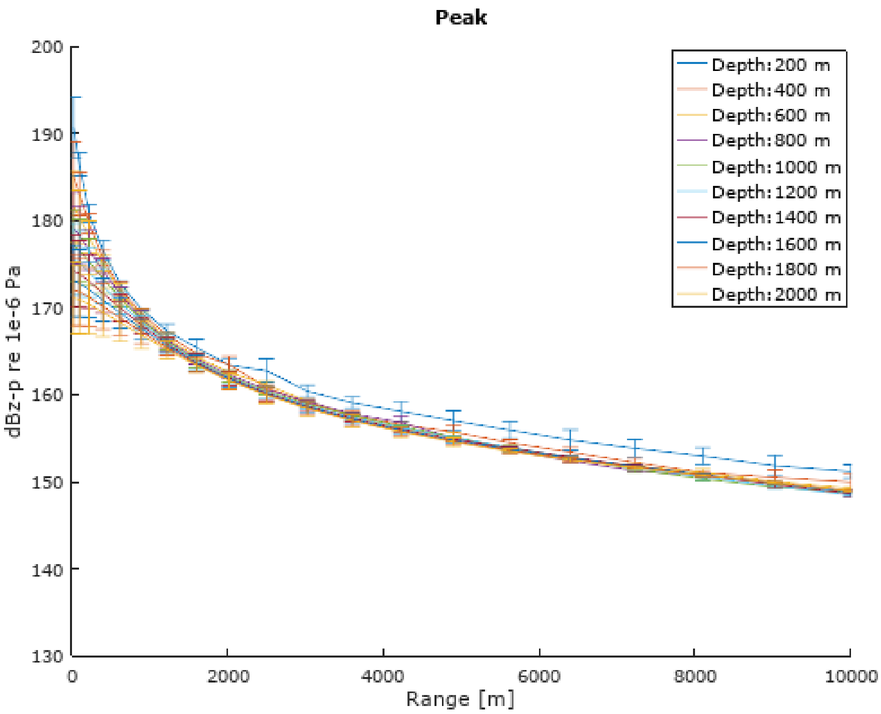

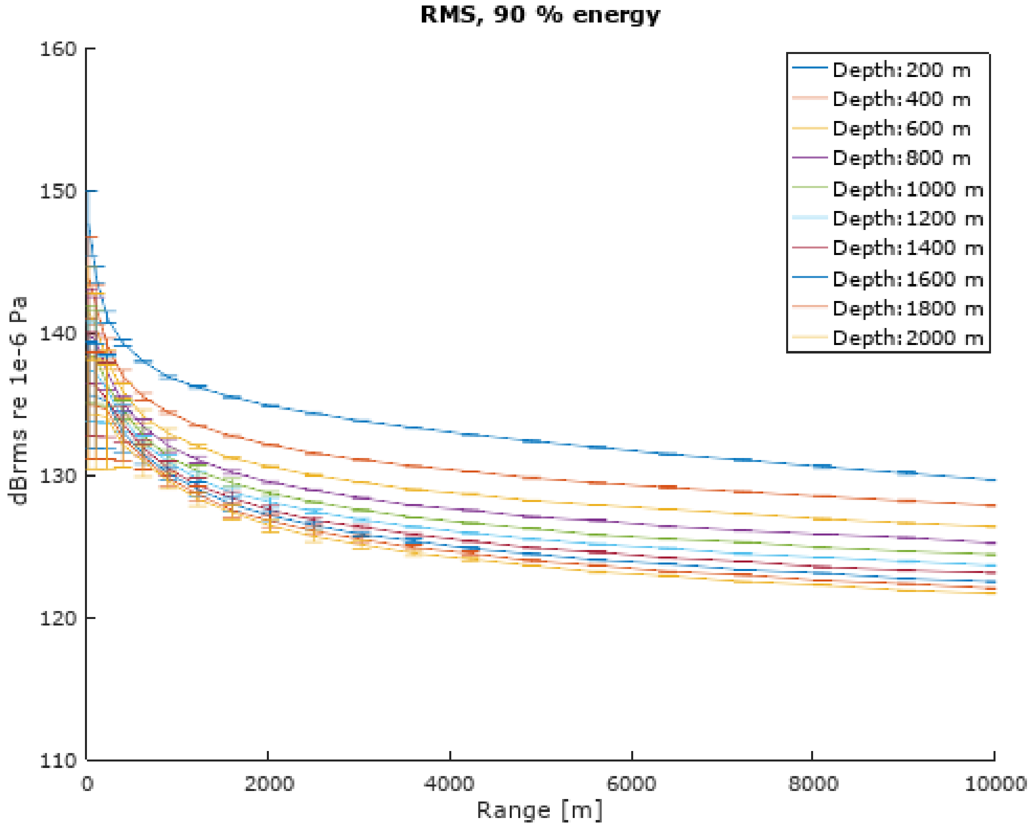
RMS, 90 % energy
dBrms re 1e-6 Pa
Range [m]
160
150
140
130
120
110
0
2000
4000
6000
8000
10000
Depth: 200 m
Depth: 400 m
Depth: 600 m
Depth: 800 m
Depth: 1000 m
Depth: 1200 m
Depth: 1400 m
Depth: 1600 m
Depth: 1800 m
Depth: 2000 m

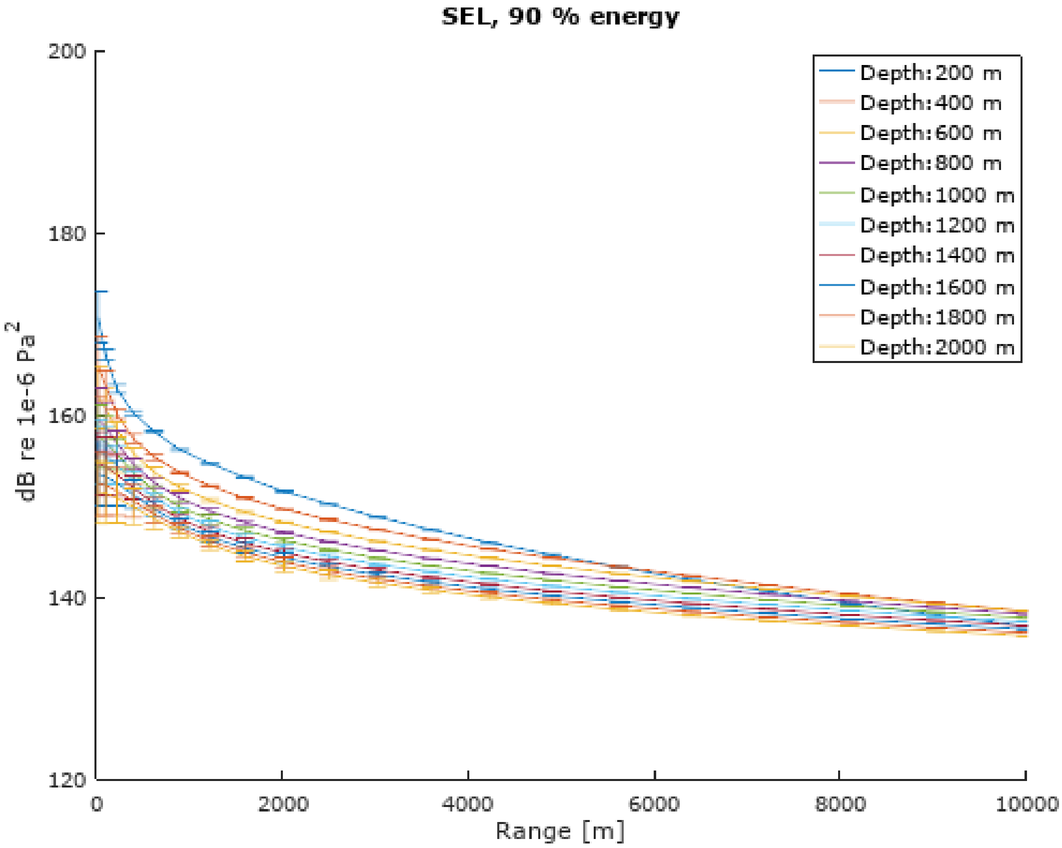
SEL, 90 % energy
dB re 1e-6 Pa^2
Range [m]
200
180
160
140
120
0
2000
4000
6000
8000
10000
Depth: 200 m
Depth: 400 m
Depth: 600 m
Depth: 800 m
Depth: 1000 m
Depth: 1200 m
Depth: 1400 m
Depth: 1600 m
Depth: 1800 m
Depth: 2000 m

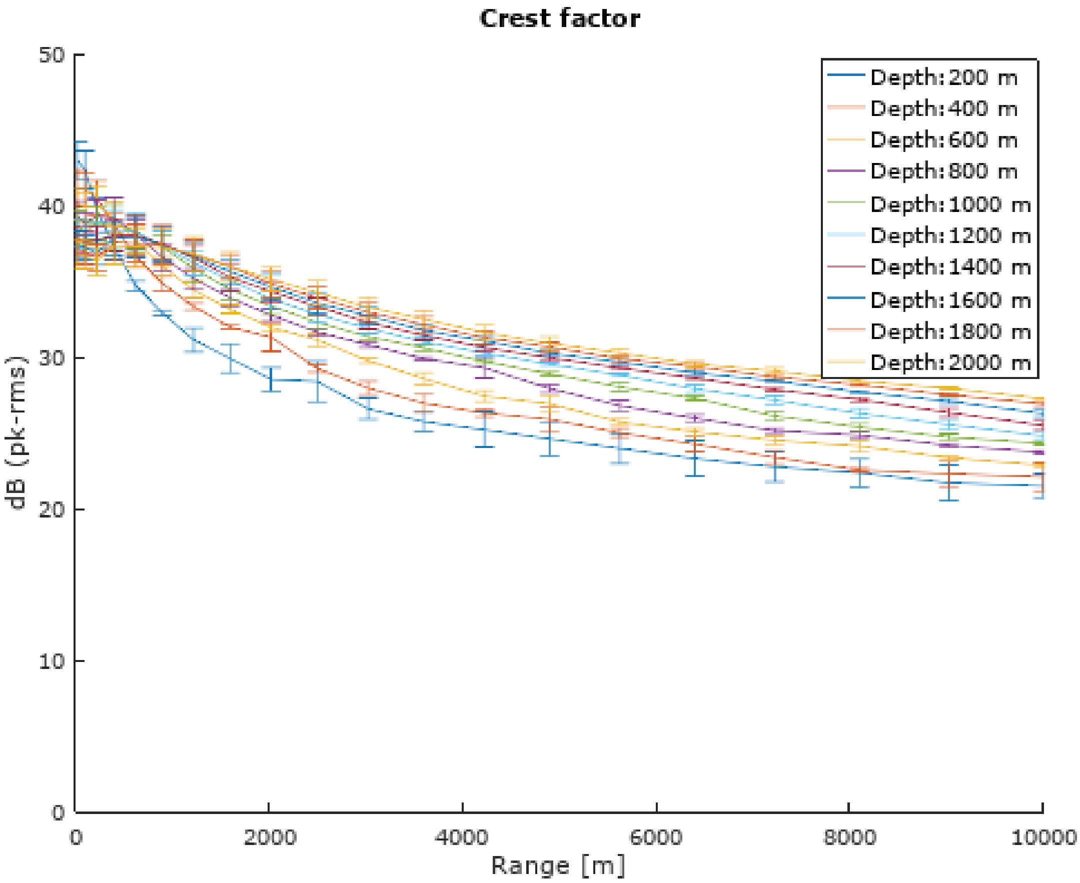
Crest factor
dB (pk-rms)
Range [m]
Depth: 200 m
Depth: 400 m
Depth: 600 m
Depth: 800 m
Depth: 1000 m
Depth: 1200 m
Depth: 1400 m
Depth: 1600 m
Depth: 1800 m
Depth: 2000 m

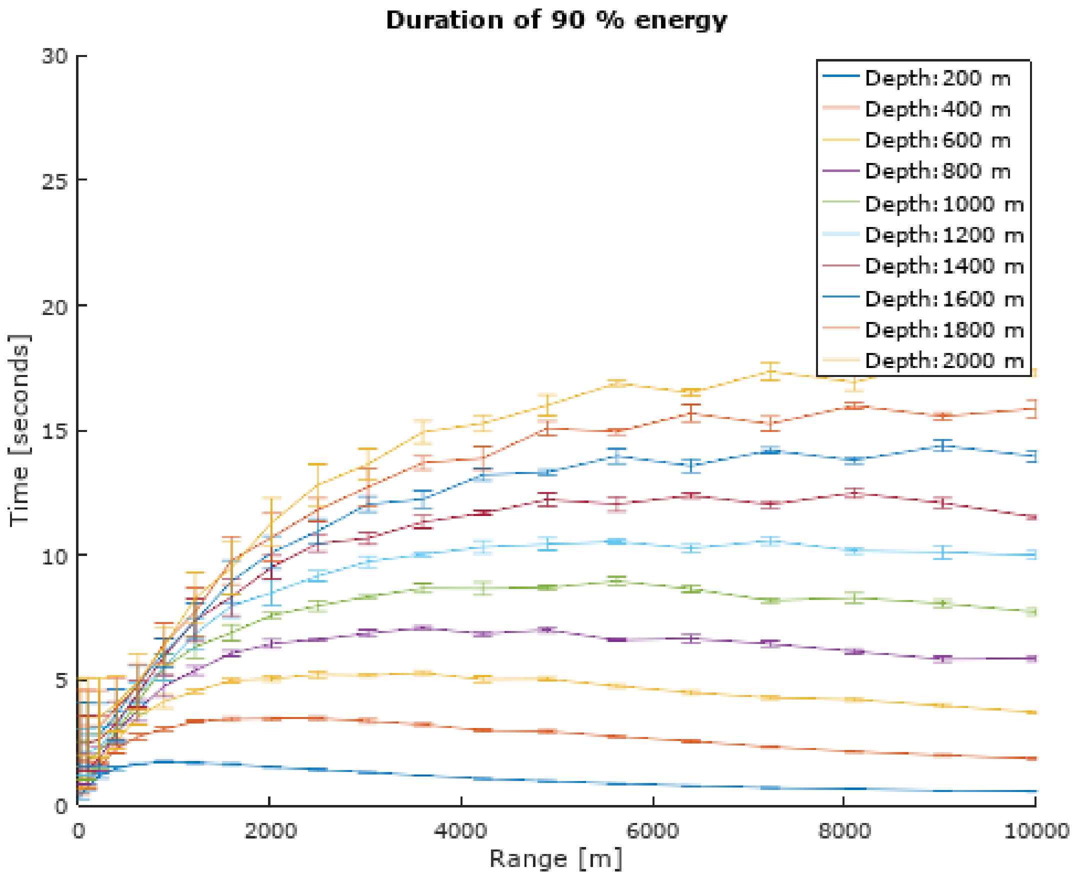
Duration of 90 % energy
Time [seconds]
Range [m]
Depth: 200 m
Depth: 400 m
Depth: 600 m
Depth: 800 m
Depth: 1000 m
Depth: 1200 m
Depth: 1400 m
Depth: 1600 m
Depth: 1800 m
Depth: 2000 m